Microwaves as a synthetic route for preparing electrochemically active TiO_2 nanoparticles

Damien Monti
Institut de Ciència de Materials de Barcelona (ICMAB-CSIC) Campus UAB, E-08193 Bellaterra, Catalonia, Spain; and Department of Applied Physics, Chalmers University of Technology, SE-41296 Gothenburg, Sweden

Alexandre Ponrouch
Institut de Ciència de Materials de Barcelona (ICMAB-CSIC) Campus UAB, E-08193 Bellaterra, Catalonia, Spain

Marc Estruga
Departament de Química, Universitat Autònoma de Barcelona, Campus UAB, E-08193 Bellaterra, Catalonia, Spain

Maria Rosa Palacín[a)]
Institut de Ciència de Materials de Barcelona (ICMAB-CSIC) Campus UAB, E-08193 Bellaterra, Catalonia, Spain

José Antonio Ayllón[b)]
Departament de Química, Universitat Autònoma de Barcelona, Campus UAB, E-08193 Bellaterra, Catalonia, Spain

Anna Roig
Institut de Ciència de Materials de Barcelona (ICMAB-CSIC) Campus UAB, E-08193 Bellaterra, Catalonia, Spain

(Received 5 May 2012; accepted 13 August 2012)

Nanocrystalline anatase was synthesized, using both domestic and laboratory microwave ovens, from different precursors. Nanoparticulate anatase was obtained after microwave irradiation of tetra-butyl orthotitanate solution in benzyl alcohol. As-synthesized samples have orange color due to the presence of organics that were eliminated after annealing at 500 °C, whereas the size of small anatase nanocrystals (around 8 nm) was preserved. Other nanocrystalline anatase samples were obtained from hexafluorotitanate-organic salt ionic liquid-like precursors. In this case, use of a domestic microwave oven and very short processing times (1–3 min irradiation time) were involved. Good specific capacity values and capacity retention at high C rates for insertion/deinsertion of Li^+ were recorded when testing such nanoparticles as electrode material in lithium cells. The electrochemical performances were found be strongly dependent on the phase composition, which in turn could be tuned through the synthetic procedure.

I. INTRODUCTION

Titanium dioxide can be considered a key technological material as it is used in a large panel of applications; also, titanium is a plentiful element, being the 10th most abundant element on the earth. Titanium dioxide is widely used as a white pigment (i.e., in paints and cosmetic products)[1] and plays a role in the biocompatibility of bone implants.[2] Other prospective applications include photocatalysis,[3,4] fuel cells,[5] solar cells,[6] sensors,[7] corrosion-protective coatings,[8,9] capacitors and thin films transistors.[10,11]

Energy storage is another most promising application for TiO_2. Anatase was tested long ago in lithium secondary cells with nonaqueous electrolytes[12] showing a flat discharge curve (~1.8 V) and quite a good cyclability but moderate reversible capacity. The feasibility of a rocking chair lithium ion battery using nanosized anatase as negative electrode was proved[13] and the electrochemical testing of other TiO_2 polymorphs in the form of nanoparticles further investigated.[14,15] TiO_2 has a theoretical specific capacity of 335 mAh/g [assuming full reduction to Ti(III) to yield lithium titanate (III) ($LiTiO_2$)] and a higher operation voltage when compared with graphite, most commonly used in batteries. This entails a severe penalty in terms of energy, which is not acceptable for portable applications. However, as the safety of lithium-ion batteries depends on the thermodynamic stability of electrode materials with respect to the electrolyte, materials operating at moderate potentials are intrinsically safer and hence most suitable for use in large-scale applications, especially for those where energy density is not the key parameter (e.g., grid). In such cases, the use of low-cost materials based on abundant and nontoxic elements is an added value, especially if suitable sustainable synthesis routes can be developed.

Microwave synthesis is becoming an increasingly attractive alternative to produce inorganic nanoparticles.[16–22] The specific microwave dielectric heating provides several advantages over other processing approaches. It is easy to operate, efficient in terms of energy and therefore is

Address all correspondence to these authors.
[a)]e-mail: rosa.palacin@icmab.es
[b)]e-mail: joseantonio.ayllon@uab.cat
DOI: 10.1557/jmr.2012.289

considered more environment-friendly.[23–25] In the case of TiO_2 the most clear advantage brought out by this route is the reduction of processing time,[26–30] other reported advantages are the production of smaller particles and differences in the polymorphs when compared with those obtained from conventional heating.[29] The microwave (MW) time reduction effect is a consequence of the enhancement in the reaction rate, due to improvements in the nucleation step.[31] Activation of adsorbed species in the growing particles may also play a significant role, as interfacial reactions are particularly susceptible to microwave irradiation.[32] Interestingly, microwave-assisted synthesis can be carried out in domestic microwave ovens,[33–35] reproducible results being achieved as long as the amount of reagents, the irradiation time and the resting periods between irradiation intervals are adequately controlled.[36–40] The use of domestic apparatus has the advantage of lower cost whereas ovens specifically designed for laboratory operation allow temperature and pressure control.[41] In some MW laboratory ovens the irradiation of the sample can be much more homogeneous than in domestic MW ovens. For the latter, the cavity exhibits regions of high energy and regions of low energy (nodes), but these inhomogeneities can be alleviated using the turning plate. Another important difference is that in domestic MW ovens the irradiation power is constant and "power control" can be achieved by switching the magnetron on and off following a duty cycle.

To the best of our knowledge no previous reports on the electrochemical testing of TiO_2 prepared using MW-based routes were available at the beginning of the present study. Two recent studies have appeared dealing with electrochemical performance of anatase prepared from titanium tetrachloride ($TiCl_4$) using a laboratory microwave-assisted solvothermal[42,43] route, but no such reports using domestic microwave ovens have yet been published.

II. EXPERIMENTAL

A. Materials

All chemicals, including tetrabutyl orthotitanate (TBOT) (Aldrich, St. Louis, MO), benzyl alcohol (Aldrich), hexafluorotitanic acid (H_2TiF_6, HFTA, 60 wt% in H_2O, Aldrich), boric acid (H_3BO_3, BA, 99%, Aldrich), triethyl ammonium chloride (TEACl, Fluka, Buchs, Switzerland), and benzyl trimethyl ammonium chloride (BTMACl, Fluka) were, at least, of reagent grade and used as received without further purification.

B. Synthetic procedure

1. TiO_2 nanoparticles synthesized using a laboratory MW oven

A 0.1 M (342 μL)TBOT solution was prepared in 10 mL of benzyl alcohol. The solution was stirred for 5 min and then placed in the microwave oven (Discover Explorer Hybrid, CEM) at 200–300 W and heated up to a selected maximum temperature (between 160 and 200 °C) for 30 min (25 min of ramping time and 5 min of heating time at the chosen temperature). The sample thus obtained was washed with ethanol and centrifuged for 20 min to remove as much benzyl alcohol as possible. The obtained powder was dried overnight at 70 °C. We have determined a minimum temperature of 185 °C to have full reaction of the precursor species. Samples were labeled as microwave anatase (MWA_T) the subindex indicating the temperature of the reaction.

2. TiO_2 nanoparticles synthesized using a domestic MW oven

Materials were prepared as previously reported.[33] Briefly, ionic liquid-like precursors were obtained by adding two equivalents of the desired organic derivative (TEACl or BTMACl) to 10 g (36.6 mmol) of HFTA solution. Precautionary steps are necessary and were taken due to the exothermic nature of the reaction and the corrosive character of the mixtures. The mixture was allowed to remain undisturbed until most of the by-product, i.e., hydrochloric acid (HCl) was lost as a vapor. Once the precursor cooled to room temperature, 1.5 equivalents of BA were added. Boric acid acted as fluoride scavenger allowing a controlled hydrolysis of the titania fluorocomplexes, leading to tetrafluoroborate (BF_4^-) anion formation and TiO_2 precipitation.[44] After BA addition, the mixture was irradiated in an open 100 mL PTFE beaker during intervals of 15 s at 800 W, using a LG Intellowave 2.45 GHz microwave oven. Two-minute resting periods were established between irradiation intervals for limiting the temperature increase. Total irradiating time was 1 min for precursor containing BTMA cation and 3 min for TEA precursor.

After the heat treatment, the crude product of the reaction was thoroughly dispersed in water by means of sonication during 5 min. Ultrapure double distilled and deionized water (Milli-Q system, Billerica, MA, conductivity lower than 0.05 μS/cm) was used in the dispersion. Then, the mixture was centrifuged at 4000 rpm to separate the solid phase. This protocol was repeated five times. Finally, the solid was dried at 85 °C overnight, producing a white compact solid that was gently milled in an agate mortar to get a white powder. Materials were labeled as domestic microwave anatase (DMW_{TEA} and DMW_{BTMA}), the subindex indicating the precursor.

3. Characterization

X-ray diffraction patterns were obtained with Siemens D-5000 (Munich, Germany) and Rigaku RU-200B diffractometers (Tokyo, Japan) using Cu $\lambda_{K\alpha}$ = 1.5418 Å

radiation. The diameter of the nanoparticles, was calculated by using the MAUD software[45] – the acronym MAUD standing for 'Materials Analysis Using Diffraction – with the Scherrer equation.[46] Thermogravimetric analysis (TGA) was performed on a TGA/SDRA 851E (Mettler Toledo, Columbus, OH) under synthetic air (mixture of 79% N_2 and 21% O_2, purity 99.996% Carburos Metálicos) in the temperature range 25–500 °C with a heating rate of 10°/min. Transmission electron micrographs (TEM) were obtained using a JEM-1210 electron microscope (JEOL Ltd., Tokyo, Japan) with an accelerating voltage of 120 kV. The sample was prepared by depositing a droplet of a dispersion of the sample in ethanol onto a holey carbon-coated copper grid.

Electrochemical tests were performed in two-electrode Swagelok cells[47] using lithium metal foil (Aldrich, 99.9%) as counter electrode. Two sheets of GF/D borosilicate glass fiber (Whatman, Kent, UK) were used as separator, soaked with 1 M hexafluoorphosphate ($LiPF_6$) in ethylene carbonate/dimethyl carbonate (1:1) electrolyte. The cells were tested using both an Arbin BT 2040 and a MacPile potentiostat (Bio-Logic, Claix, France) through galvanostatic cycling with potential limitation (GCPL) experiments. The voltage window was 1–3 V. The rate was set at C/15 for powdered electrodes whereas different rates from C/15 to 2C were used for film electrodes (where C/n is equivalent to 1 mol of lithium atoms per formula unit within n hours). The working electrode consisted either of a powdered mixture containing 80% of TiO_2 with 20% of carbon black (Super P, Timcal, Bodio, Switzerland) or a 0.8 cm^2 disk composite tape electrode. The later were prepared from slurries [65 wt% TiO_2, 8 wt% of polyvinylidene fluoride binder (PVDF; Arkema, Colombes, France) and 27 wt% of Super P carbon in *N*-methylpyrrolidone (NMP; Aldrich)] mixed for 15 h by magnetic stirring with three intermediate 10-min sonication steps.[48] These were tape-cast on a 20-μm thick copper foil (Goodfellow, Huntingdon, UK) with a 250-μm Doctor-Blade and further dried at 120 °C under vacuum prior to pressing at 8 tons.

III. RESULTS AND DISCUSSION

A. Materials synthesis and characterization

In the case of the laboratory microwave synthesis, benzyl alcohol was chosen as a solvent as it is environmentally friendly and has proved to be very useful for the synthesis of different transition metal oxide nanoparticles.[49,50] Patterns (a) and (b), in Fig. 1, correspond to MWA_{185} and MWA_{200} as-prepared samples. The former is poorly crystallized and exhibits very broad peaks, which are much better defined for the latter. All observed reflections correspond to anatase and the calculated crystallite sizes are in nanometric range, around 8 nm. The as-obtained MWA powders were orange in color, indicating the presence of adsorbed organics. TGA curve coupled with its

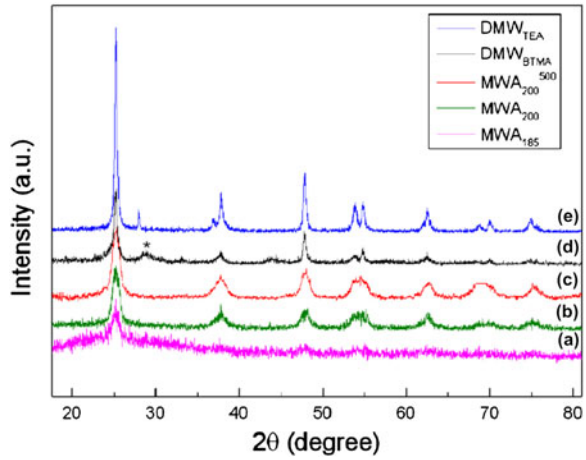

FIG. 1. XRD pattern of MWA_{185} (a), MWA_{200} (b), MWA_{200}^{500} (c), DMW_{BTMA} (d), DMW_{TEA} (e) with peaks ascribed to TiO_2-B(*).

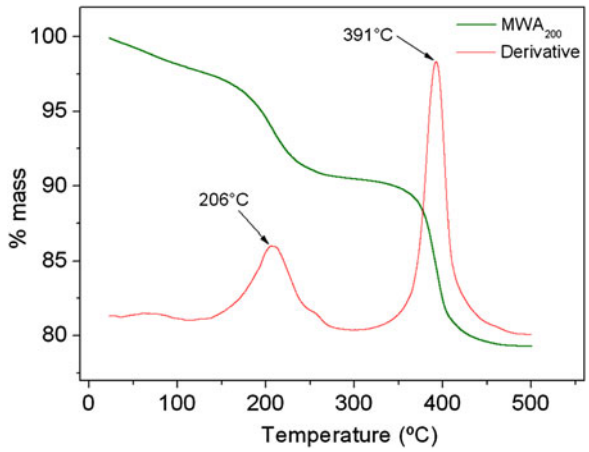

FIG. 2. TGA curve for MWA_{200} and its derivative.

derivative (Fig. 2) exhibits a first 10% mass loss centered around 206 °C ascribed to organic volatile compounds and a second 10% weight loss around 391 °C presumably probably due to benzyl alcohol degradation products strongly adsorbed on TiO_2 surface. The sample turned white after heat treatment at 500 °C in agreement with the remaining organics being responsible for the orange color. Sample MWA_{200} was thus further annealed at 500 °C (MWA_{200}^{500}) to eliminate remaining organics. XRD pattern [Fig. 1(c)] confirms that the anatase polymorph was preserved after annealing.

Transmission electron micrographs show that the as-made MWA_{200} sample [Fig. 3(a)] consists of particles with a size ranging between 4 and 15 nm consistent with the values derived from x-ray diffraction data, wrapped in a sort of gel that we ascribe to the organic matter, which prevented them from aggregating. After heat treatment, in MWA_{200}^{500} the particle size is roughly preserved, but the elimination of the organic matter has led to the formation of aggregates [Fig. 3(b)].

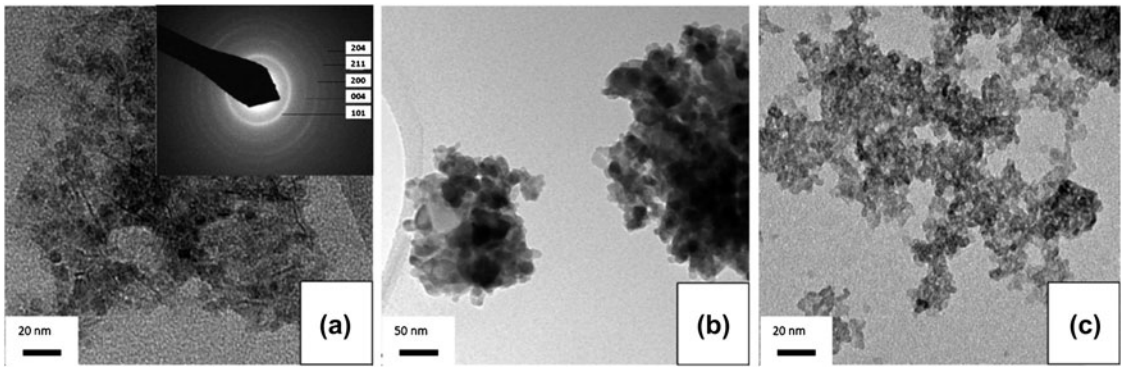

FIG. 3. TEM micrographs of anatase synthesized using a laboratory MW oven: MWA_{200} (a), MWA_{200}^{500} (b), and a domestic microwave DMW_{BTMA} (c).

In the case of the domestic oven, we have attempted to use precursors that would yield pure TiO_2 free of organics and to choose salts consisting of an organic cation and the hexafluorotitanate anion. The conversion of these precursors to TiO_2 has been previously found to progress effectively using MW radiation and boric acid as fluoride scavenger. Nanocrystalline anatase was obtained after 3 min of MW treatment for both precursors [see Figs. 1(d) and 1(e)], the estimated crystallite sizes being 28 and 20 nm for DMW_{TEA} and DMW_{BTMA} respectively. Samples were not subjected to any further thermal treatment. A closer look at the XRD pattern allowed identifying a certain amount of TiO_2-B in these samples, higher for DMW_{BTMA} prepared from BTMA (see Fig. 1). Transmission electron micrographs for DMW_{BTMA} [Fig. 3(c)] consist of disperse particles with a size ranging between 4 and 10 nm, similar to MWA_{200}.

B. Electrochemical characterization

The redox reaction mechanism reported for anatase[13,51–54] is found to consist of three distinct steps. First, an initial monotonous potential decrease is observed corresponding to lithium insertion into the empty octahedral sites within the anatase structure through a single-phase process forming $Li_{\varepsilon}TiO_2$. Second, a plateau is observed at ~1.8 V corresponding to a two-phase process involving the formation of $Li_{0.5}TiO_2$ whereas a sloppy region is observed after the plateau, which has been found to increase with increasing surface area of the samples and to have a significant capacitive-like contribution.

Figures 4 and 5 exhibit the voltage versus composition profile and capacity versus cycle number for all the studied samples when tested using powder electrode technology, which is consistent with what would be expected for anatase. Still, some differences are observed between the samples. The three regions are clearly distinct for MWA_{200} with the initial solid solution range extending to $\varepsilon = 0.087$, the plateau ending at $Li_{0.45}TiO_2$ and overall Δx value close to 0.8 (268 mAh/g).

There is a significant irreversible capacity on the first cycle ($\Delta x_{irr} = 0.18$) but capacities are maintained afterward (~200 mAh/g) with some slow fading. The sample annealed at 500 °C (MWA_{200}^{500}) exhibits a similar profile but with a much smaller solid solution degree ($\varepsilon = 0.056$) and smaller overall capacity on the first cycle (Δx value close to 0.59, 170 mAh/g) but also smaller irreversible capacity ($\Delta x_{irr} = 0.08$) and much lower capacity fading (45% after 20 cycles for MWA_{200} compared with 8% for MWA_{200}^{500}). This would be in agreement with some irreversible capacity for MWA_{200} being due to reduction of the remaining organics. The outcome of such organics upon cycling is difficult to ascertain, as in addition to being reduced/decomposed they may even be dissolved in the electrolyte, yet, it seems clear that their presence is detrimental for capacity retention.

Samples prepared using the domestic microwave (DMW_{TEA} and DMW_{BTMA}) exhibit much less defined plateaux, especially for the latter, prepared from DMW_{BTMA}. These profiles are much closer to those reported for TiO_2-B[55,56] than to the typical behavior of anatase. This similarity was further confirmed by preparing nanometric TiO_2-B according to Estruga et al.[57] and testing them electrochemically under the same conditions used for DMW_{TEA} and DMW_{BTMA}. The reason behind this behavior is unclear at this stage, as such a profile would not be expected if the sample were a biphasic mixture of anatase and TiO_2-B particles. The most plausible hypothesis at this time is that the sample is constituted of biphasic particles and that the small fraction of TiO_2-B constitutes the particles' outer surface layer and hence dominates the electrochemical response. Still, further investigations are being undertaken to ascertain this point. Correlation of microstructure/phase composition with electrochemical performance for such samples would help in ascertaining the reasons behind the good performance achieved for DMW_{BTMA}.

With the aim of determining both performance at high rates and capacity fading, tests on the samples exhibiting higher capacities (DMW_{TEA} and DMW_{BTMA}) were also

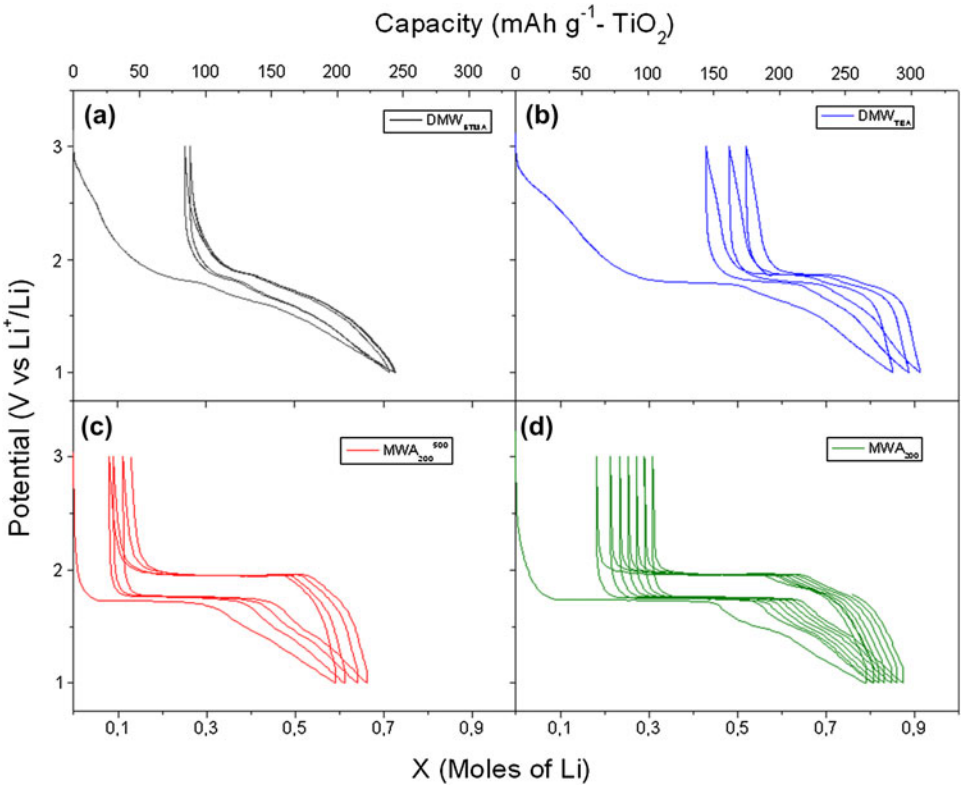

FIG. 4. Potential versus composition and capacity profile for DMW_{BTMA} (a), DMW_{TEA} (b) MWA_{200}^{500} (c), MWA_{200} (d), cycled at C/15-rate.

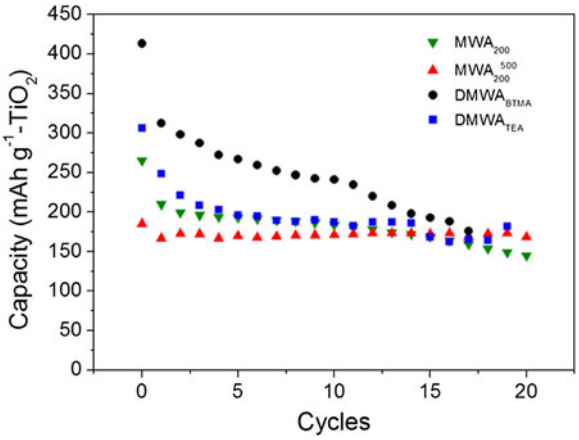

FIG. 5. Capacity versus cycle number for MWA_{200} (green inverted triangles), MWA_{200}^{500} (red triangles), DMW_{BTMA} (black circles), DMW_{TEA} (blue squares) cycled at C/15-rate.

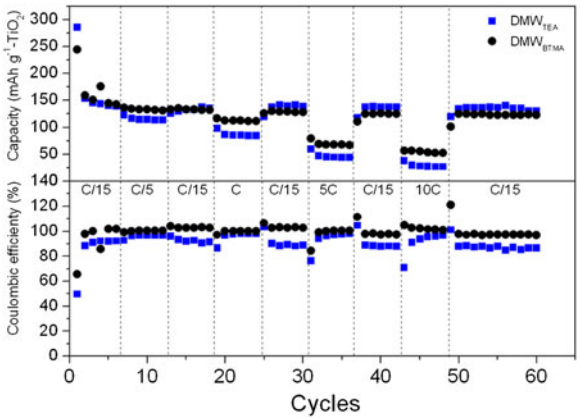

FIG. 6. Capacity versus cycle number of DMW_{BTMA} (black circles) and DMW_{TEA} (blue squares).

made using a tape electrode technology very similar to industrial electrode fabrication processes. Electrodes were overall tested at C/15 for ~60 cycles with intercalated cycling steps at higher rates ranging from C/5 to 10C. Figure 6 exhibits the capacity versus cycle number for such tests.

DMW_{BTMA} and DMW_{TEA} exhibit initial capacities of 285 and 243 mAh/g at C/15 but undergo significant losses upon the first set of cycles. Overall, capacities tend to stabilize to values close to 140 mAh/g, which are similar, though slightly lower, than those recently reported for nanosized anatase made through a microwave-assisted solvothermal route.[42,43] Still, the coulombic efficiencies upon cycling are close to 100% (being higher for DMW_{BTMA} containing TiO_2-B). The rate capability for both samples is found to be rather good and again, higher for DMW_{BTMA}. Indeed, capacity values of ~70 and 45 mAh/g were recorded at 5C for DMW_{BTMA} and DMW_{TEA}, respectively (i.e., 50% and 32% of the full capacity recorded at C/15). While it is known

that electrochemical performance at such high rates will certainly be dependent on electrode processing,[58] no specific optimization study for electrode formulation was carried out; these capacity values are somewhat lower than those reported for mesoporous anatase TiO_2 nano networks[59,60] but within the same order of magnitude of those reported for nanosized anatase prepared using alternative methods and tested under similar conditions.[61]

For a better understanding of the good performances in terms of capacity retention at high C rates observed in the case of DMW_{BTMA}, potential versus capacity profiles at C rates ranging from C/15 to 5C were plotted for both DMW_{TEA} and DMW_{BTMA}. The results are shown in Fig. 7 and capacity values were normalized for sake of clarity. A much higher voltage hysteresis between charge and discharge is observed for DMW_{TEA} tape-cast electrodes cycled at high C rates as compared with DMW_{BTMA} based electrodes. This can also be seen by comparison of the overpotential values at the end of discharge [see inset in Figs. 7(a) and 7(b)], being as high as 100 mV at 5C for DMW_{TEA}. By contrast, only ~46 mV overpotential is recorded at the same C rate for DMW_{BTMA}, indicating a better electronic and/or ionic conductivity when BTMA is used as a precursor. It is hypothesized that the presence of TiO_2-B in BTMA favored the ionic conductivity of Li^+ inside the particles, due to its structure being more open than other polymorphs, with a density of 3.73 g/cm^3 compared with 3.89 g/cm^3 for anatase and hence allowing easier Li^+ transport[15] but further studies are needed to ascertain this point. Overpotential contributions have dramatic consequences on the capacity retention for systems with a redox mechanism entailing an almost linear potential decay at low potential values and should thus be avoided by manipulation of (i) the electrode formulation for reducing the ohmic drop contribution as much as possible and (ii) the phase composition so as to improve Li^+ diffusion. The appearance of an additional oxidation feature visible for DMW_{BTMA} when the C rate is increased [see Fig. 7(a), red arrow] is also worth mentioning. It is found that such feature shifts to higher potential values when the C rate is increased and disappears when the C rate is decreased down to C/15. This observation is consistent with the presence of two distinct electrochemical processes with different kinetics, the one occurring at higher potential being slower. Research is currently underway for optimizing the synthesis parameters allowing tuning the proportion of the different TiO_2 polymorphs in the samples and hence a more fundamental study on the electrochemical response.

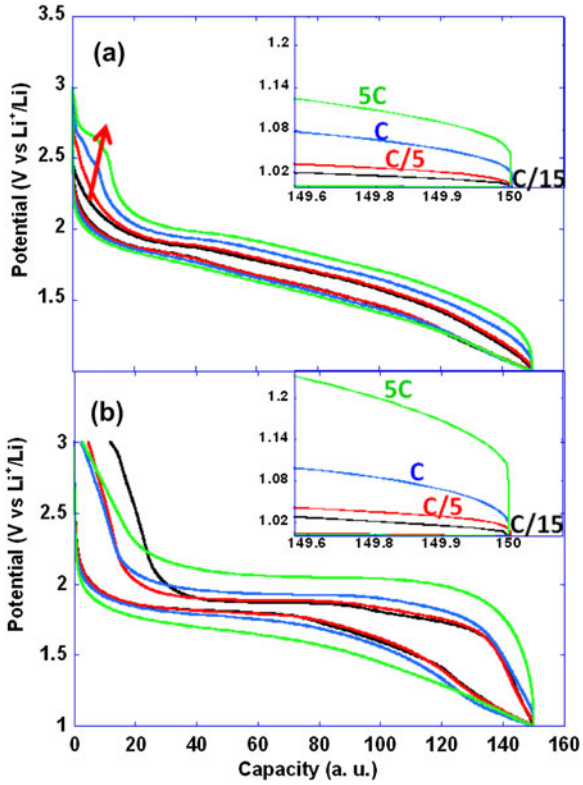

FIG. 7. Normalized voltage versus capacity profiles for (a) DMW_{TEA} and (b) DMW_{BTMA}, cycled at C rates of C/15, C/5, C, and 5C. Insets display zoomed plot of the overpotential visible between charge and discharge.

IV. CONCLUSIONS

The use of microwave radiation was demonstrated as a successful synthetic technique to yield nanocrystalline TiO_2 with laboratory and domestic dedicated microwave ovens. The short exposition times (only ~1–3 min) provided small particle size (5–15 nm) interesting for electrochemistry. Good electrochemical performances were recorded for such nanoparticles with stable specific capacity values of more than approximately 140 mAh/g at C/15 and good capacity retention at high C rates (70 mAh/g at 5C). The fact that samples are not pure anatase but do also contain some TiO_2-B may indicate that diverse polymorphs can also be obtained using domestic ovens, as reported for laboratory ovens, through control of precursors and synthesis conditions. These results clearly prove that microwave synthesis is an appealing route to obtain nanometric TiO_2 with good electrochemical performance.

ACKNOWLEDGMENTS

We acknowledge Patrik Johansson for valuable discussions and are grateful to Ministerio de Ciencia e Innovación (Spain) for Grant Nos. MAT2011-24757, MAT2009-08024 and Nanoselect-CSD2007-00041 and the Generalitat de Catalunya for Grant No. 2009SGR-203.

REFERENCES

1. N. Gussman: We're history - titanium dioxide: From black sand to white pigment. *Chem. Eng. Prog.* **101**, 64 (2005).

2. L. Rasmusson, J. Roos, and H. Bystedt: A 10-year follow-up study of titanium dioxide-blasted implants. *Clin. Implant Dent. R.* **7**, 36 (2005).
3. A. Fujishima and X.T. Zhang: Titanium dioxide photocatalysis: Present situation and future approaches. *C.R. Chim.* **9**, 750 (2006).
4. M.A. Henderson: A surface science perspective on TiO_2 photocatalysis. *Surf. Sci. Rep.* **66**, 185 (2011).
5. Y. Qiao, S.J. Bao, C.M. Li, X.Q. Cui, Z.S. Lu, and J. Guo: Nanostructured polyaniline/titanium dioxide composite anode for microbial fuel cells. *ACS Nano* **2**, 113 (2008).
6. L.M. Peter: The Gratzel cell: Where next? *J. Phys. Chem. Lett.* **2**, 1861 (2012).
7. S.J. Yuan, R.Y. Mao, Y.G. Li, Q.H. Zhang, and H.Z. Wang: Layer-by-layer assembling TiO_2 film from anatase TiO_2 sols as the photoelectrochemical sensor for the determination of chemical oxygen demand. *Electrochim. Acta* **60**, 347 (2012).
8. J.H. Hu, S.K. Guan, C.L. Zhang, C.X. Ren, C.L. Wen, Z.Q. Zeng, and L. Peng: Corrosion protection of AZ31 magnesium alloy by a TiO_2 coating prepared by LPD method. *Surf. Coat. Technol.* **203**, 2017 (2009).
9. C.X. Lei, H. Zhou, Z.D. Feng, Y.F. Zhu, and R.G. Du: Liquid phase deposition (LPD) of TiO_2 thin films as photoanodes for cathodic protection of stainless steel. *J. Alloys Compd.* **513**, 552 (2012).
10. S. Chao and F. Dogan: Processing and dielectric properties of TiO_2 thick films for high-energy density capacitor applications. *Int. J. Appl. Ceram. Technol.* **8**, 1363 (2011).
11. L.A. Majewski, R. Schroeder, and M. Grell: Low-voltage, high-performance organic field-effect transistors with an ultrathin TiO_2 layer as gate insulator. *Adv. Funct. Mater.* **15**, 1017 (2005).
12. T. Ohzuku, Z. Takehara, and S. Yoshizawa: Nonaqueous lithium-titanium dioxide cell. *Electrochim. Acta* **24**, 219 (1979).
13. S.Y. Huang, L. Kavan, I. Exnar, and M. Gratzel: Rocking chair lithium battery based on nanocrystalline TiO_2 (anatase). *J. Electrochem. Soc.* **142**, L142 (1995).
14. X. Su, Q.L. Wu, X. Zhan, J. Wu, S.Y. Wei, and Z.H. Guo: Advanced titania nanostructures and composites for lithium ion battery. *J. Mater. Sci.* **47**, 2519 (2012).
15. Z.G. Yang, D. Choi, S. Kerisit, K.M. Rosso, D.H. Wang, J. Zhang, G. Graff, and J. Liu: Nanostructures and lithium electrochemical reactivity of lithium titanites and titanium oxides: A review. *J. Power Sources* **192**, 588 (2009).
16. J. Chen, J. Wang, X. Zhang, and Y.L. Jin: Microwave-assisted green synthesis of silver nanoparticles by carboxymethyl cellulose sodium and silver nitrate. *Mater. Chem. Phys.* **108**, 421 (2008).
17. R.G. Deshmukh, S.S. Badadhe, and I.S. Mulla: Microwave-assisted synthesis and humidity sensing of nanostructured alpha-Fe_2O_3. *Mater. Res. Bull.* **44**, 1179 (2009).
18. M. Godinho, C. Ribeiro, E. Longo, and E.R. Leite: Influence of microwave heating on the growth of gadolinium-doped cerium oxide nanorods. *Cryst. Growth Des.* **8**, 384 (2008).
19. A.L. Washington and G.F. Strouse: Microwave synthesis of CdSe and CdTe nanocrystals in nonabsorbing alkanes. *J. Am. Chem. Soc.* **130**, 8916 (2008).
20. X.W. Zheng, Q.T. Hu, and C.S. Sun: Efficient rapid microwave-assisted route to synthesize InP micrometer hollow spheres. *Mater. Res. Bull.* **44**, 216 (2009).
21. O. Pascu, J.M. Caicedo, M. Lopez-Garcia, V. Canalejas, A. Blanco, C. Lopez, J. Arbiol, J. Fontcuberta, A. Roig, and G. Herranz: Ultrathin conformal coating for complex magnetophotonic structures. *Nanoscale* **3**, 4811 (2011).
22. O. Pascu, E. Carenza, M. Gich, S. Estradé, F. Peiré, G. Herranz, and A. Roig: Surface reactivity of iron oxide nanoparticles by microwave-assisted synthesis; comparison with the thermal decomposition route. *J. Phys. Chem. C* **116**, 15108 (2012).
23. D.M.P. Mingos and D.R. Baghurst: Applications of microwave dielectric heating effects to synthetic problems in chemistry. *Chem. Soc. Rev.* **20**, 1 (1991).
24. I. Bilecka and M. Niederberger: Microwave chemistry for inorganic nanomaterials synthesis. *Nanoscale* **2**, 1358 (2010).
25. D. Stuerga, K. Gonon, and M. Lallemant: Microwave-heating as a new way to induce selectivity between competitive reactions - application to isomeric ratio control in sulfonation of naphthalene. *Tetrahedron* **49**, 6229 (1993).
26. M. Addamo, M. Bellardita, D. Carriazo, A. Di Paola, S. Milioto, L. Palmisano, and V. Rives: Inorganic gels as precursors of TiO_2 photocatalysts prepared by low-temperature microwave or thermal treatment. *App. Catal., B* **84**, 742 (2008).
27. I. Bilecka, I. Djerdj, and M. Niederberger: One-minute synthesis of crystalline binary and ternary metal oxide nanoparticles. *Chem. Commun.* **7**, 886 (2008).
28. C.C. Chung, T.W. Chung, and T.C.K. Yang: Rapid synthesis of titania nanowires by microwave-assisted hydrothermal treatments. *Ind. Eng. Chem. Res.* **47**, 2301 (2008).
29. F. Dufour, S. Cassaignon, O. Durupthy, C. Colbeau-Justin, and C. Chanéac: Do TiO_2 nanoparticles really taste better when cooked in a microwave oven? *Eur. J. Inorg. Chem.* **16**, 2707 (2012).
30. E. Gressel-Michel, D. Chaumont, and D. Stuerga: From a microwave flash-synthesized TiO_2 colloidal suspension to TiO_2 thin films. *J. Colloid Interface Sci.* **285**, 674 (2005).
31. S.H. Jhung, T.H. Jin, Y.K. Hwang, and J.S. Chang: Microwave effect in the fast synthesis of microporous materials: Which stage between nucleation and crystal growth is accelerated by microwave irradiation? *Chem. Eur. J.* **13**, 4410 (2007).
32. W.C. Conner and G.A. Tompsett: How could and do microwaves influence chemistry at interfaces? *J. Phys. Chem. B* **112**, 2110 (2008).
33. M. Estruga, C. Domingo, and J.A. Ayllon: Microwave radiation as heating method in the synthesis of titanium dioxide nanoparticles from hexafluorotitanate-organic salts. *Mater. Res. Bull.* **45**, 1224 (2010).
34. X.T. Jia, W. He, X.D. Zhang, H.S. Zhao, Z.M. Li, and Y.J. Feng: Microwave-assisted synthesis of anatase TiO_2 nanorods with mesopores. *Nanotechnology* **18**, 075602 (2007).
35. V.G. Pol, Y. Langzam, and A. Zaban: Application of microwave superheating for the synthesis of TiO_2 rods. *Langmuir* **23**, 11211 (2007).
36. K.L. Ding, Z.J. Miao, Z.M. Liu, Z.F. Zhang, B.X. Han, G.M. An, S.D. Miao, and Y. Xie: Facile synthesis of high quality TiO_2 nanocrystals in ionic liquid via a microwave-assisted process. *J. Am. Chem.Soc.* **129**, 6362 (2007).
37. H.M.A. Hassan, V. Abdelsayed, A.E.R.S. Khder, K.M. AbouZeid, J. Terner, M.S. El-Shall, S.I. Al-Resayes, and A.A. El-Azhary: Microwave synthesis of graphene sheets supporting metal nanocrystals in aqueous and organic media. *J. Mater. Chem.* **19**, 3832 (2009).
38. D.S. Jacob, I. Genish, L. Klein, and A. Gedanken: Carbon-coated core shell structured copper and nickel nanoparticles synthesized in an ionic liquid. *J. Phys. Chem. B* **110**, 17711 (2006).
39. C. Parada and E. Moran: Microwave-assisted synthesis and magnetic study of nanosized Ni/NiO materials. *Chem. Mater.* **18**, 2719 (2006).
40. C. Yacou, M.L. Fontaine, A. Ayral, P. Lacroix-Desmazes, P.A. Albouy, and A. Julbe: One pot synthesis of hierarchical porous silica membrane material with dispersed Pt nanoparticles using a microwave-assisted sol-gel route. *J. Mater. Chem.* **18**, 4274 (2008).
41. C.O. Kappe: Controlled microwave heating in modern organic synthesis. *Angew. Chem. Int. Ed.* **43**, 6250 (2004).
42. S. Yoon, E-S. Lee, and A. Manthiram: Microwave-solvothermal synthesis of various polymorphs of nanostructured TiO_2 in different

alcohol media and their lithium ion storage properties. *Inorg. Chem.* **51**, 3505 (2012).
43. D. Zhang, M. Wen, P. Zhang, J. Zhu, G. Li, and H. Li: Microwave-induced synthesis of porous single-crystal-like TiO_2 with excellent lithium storage properties. *Langmuir* **28**, 4543 (2012).
44. S. Deki, Y. Aoi, O. Hiroi, and A. Kajinami: Titanium (IV) oxide thin films prepared from aqueous solution. *Chem. Lett.* **25**, 433 (1996).
45. J. Rodriguez-Carvajal: Recent advances in magnetic structure determination by neutron powder diffraction. *Physica B* **192**, 55 (1993).
46. W.N. Schreiner and R. Jenkins: Profile fitting for quantitative analysis in x-ray-powder diffraction. *Adv. X-Ray Anal.* **26**, 141 (1983).
47. D. Guyomard and J.M. Tarascon: Li metal-free rechargeable $LiMn_2O_4$/carbon cells - their understanding and optimization. *J. Electrochem. Soc.* **139**, 937 (1992).
48. A. Ponrouch and M.R. Palacin: On the impact of the slurry mixing procedure in the electrochemical performance of composite electrodes for Li-ion batteries: A case study for mesocarbon microbeads (MCMB) graphite and Co_3O_4. *J. Power Sources* **196**, 9682 (2011).
49. M. Niederberger, M.H. Bard, and G.D. Stucky: Benzyl alcohol and transition metal chlorides as a versatile reaction system for the nonaqueous and low-temperature synthesis of crystalline nano objects with controlled dimensionality. *J. Am. Chem. Soc.* **24**, 13642 (2002).
50. M. Niederberger, M.H. Bartl, and G.D. Stucky: Benzyl alcohol and titanium tetrachloride - a versatile reaction system for the nonaqueous and low-temperature preparation of crystalline and luminescent titania nanoparticles. *Chem. Mater.* **14**, 4364 (2002).
51. C.H. Jiang, M.D. Wei, Z.M. Qi, T. Kudo, I. Honma, and H.S. Zhou: Particle size dependence of the lithium storage capability and high-rate performance of nanocrystalline anatase TiO_2 electrode. *J. Power Sources* **166**, 239 (2007).
52. A. Stashans, S. Lunell, R. Bergstrom, A. Hagfeldt, and S.E. Lindquist: Theoretical study of lithium intercalation in rutile and anatase. *Phys. Rev. B* **53**, 159 (1996).
53. G. Sudant, E. Baudrin, D. Larcher, and J.M. Tarascon: Electrochemical lithium reactivity with nanotextured anatase-type TiO_2. *J. Mater. Chem.* **15**, 1263 (2005).
54. M. Wagemaker, W.J.H. Borghols, and F.M. Mulder: Large impact of particle size on insertion reactions. A case for anatase Li_xTiO_2. *J. Am. Chem. Soc.* **129**, 4323 (2007).
55. P.G. Bruce: Energy storage beyond the horizon: Rechargeable lithium batteries. *Solid State Ionics* **179**, 752 (2008).
56. Y. Ren, Z. Liu, F. Pourpoint, A.R. Armstrong, C.P. Grey, and P.G. Bruce: Nanoparticulate TiO_2(B): An anode for lithium-ion batteries. *Angew. Chem. Int. Ed.* **51**, 2164 (2012).
57. M. Estruga, C. Domingo, and J.A. Ayllon: Low-temperature and ambient-pressure synthesis of TiO_2-B. *Mater. Lett.* **64**, 2357 (2010).
58. E. Ligneel, B. Lestriez, O. Richard, and D. Guyomard: Optimizing lithium battery performance from a tailor-made processing of the positive composite electrode. *J. Phys. Chem. Solids* **67**, 1275 (2006).
59. H.G. Jung, S.W. Oh, J. Ce, N. Jayaprakash, and Y.K. Sun: Mesoporous TiO_2 nanonetworks: Anode for high-power lithium battery applications. *Electrochem. Comm.* **11**, 756 (2009).
60. P. Kubiak, T. Fröschl, N. Hüsing, U. Hörmann, U. Kaiser, R. Schiller, C.K. Weiss, K. Landfester, and M. Wohlfahrt-Mehrens: TiO_2 anatase nanoparticle networks: Synthesis, structure and electrochemical performance. *Small* **7**, 1690 (2011).
61. H.E. Wang, H. Cheng, C. Liu, X. Chen, A. Jiang, Z. Lu, Y.Y. Li, C.Y. Chung, W. Zhang, J.A. Zapien, L. Martinu, and I. Bello: Facile synthesis and electrochemical characterization of porous and dense TiO_2 nanospheres for lithium-ion battery applications. *J. Power Sources* **196**, 6394 (2011).

Supplementary Material

Supplementary material can be viewed in this issue of the *Journal of Materials Research* by visiting http://journals.cambridge.org/jmr.